ICASE-84-5

NASA Contractor Report 172300

NASA-CR-172300
19840011217

ICASE

ON THE STABILITY OF AN INFINITE SWEPT
ATTACHMENT LINE BOUNDARY LAYER

P. Hall

M. R. Malik

D. I. A. Poll

INSTITUTE FOR COMPUTER APPLICATIONS IN SCIENCE AND ENGINEERING
NASA Langley Research Center, Hampton, Virginia 23665

Operated by the Universities Space Research Association

NASA

National Aeronautics and
Space Administration

Langley Research Center
Hampton, Virginia 23665

ON THE STABILITY OF AN INFINITE SWEPT

ATTACHMENT LINE BOUNDARY LAYER

P. Hall
Imperial College, London, England

M. R. Malik
High Technology Corporation
P. O. Box 7262, Hampton, VA 23666

D. I. A. Poll
College of Aeronautics, Cranfield, England

Abstract

The instability of an infinite swept attachment line boundary layer is considered in the linear regime. The basic three-dimensional flow is shown to be susceptible to travelling wave disturbances which propagate along the attachment line. The effect of suction on the instability is discussed and the results suggest that the attachment line boundary layer on a swept wing can be significantly stabilized by extremely small amounts of suction. The results obtained are in excellent agreement with the available experimental observations.

i

N84-19285

INTRODUCTION

The laminar boundary layer which forms on a long cylinder whose axis is inclined relative to the oncoming flow is known to exhibit instability to small amplitude disturbances at large Reynolds numbers. Depending upon the flow conditions these disturbances may take the form of Tollmien-Schlichting waves, stationary cross-flow vortices or, if the surface has regions of concave curvature, Taylor-Görtler vortices. In general, as the Reynolds number is increased, the instability occurs first in the regions of adverse pressure gradient on the lee side of the cylinder. Further increases in Reynolds number cause the location of the instability to move progressively forward towards the attachment line. It follows that the Reynolds number at which the attachment line flow exhibits an instability to small amplitude disturbances represents a limit beyond which the flow over the cylinder is unstable everywhere.

The motivation for studying the flow over inclined cylinders lies in the fact that the results find direct application in situations of engineering significance, notably to the flow over high aspect ratio swept back wings. In recent years the attempted development of laminar flow wings has resulted in renewed interest in the instability mechanisms which can affect a three-dimensional laminar boundary layer. For conventional wings operating at typical long range cruise conditions a laminar boundary layer would be unstable over a large proportion of the surface area and, consequently, wholly laminar flow cannot be maintained without the use of some form of artificial stability augmentation. The most convenient form of stabilization is that provided by distributed surface suction. Surface suction affects the boundary layer in two ways. Firstly, the viscous layer is thinned with a corresponding

reduction in local Reynolds number. Secondly, and more importantly, the vorticity distribution within the boundary layer is modified in such a way that a more stable flow is established. The combination of these separate effects makes surface suction a particularly efficient stabilization mechanism with transpiration velocities of order .1% of the velocity at the edge of the boundary layer being sufficient to maintain aerofoil boundary layers in the laminar state. Therefore, an investigation of the stability characteristics of the attachment line boundary layer with and without surface transpiration constitutes a problem of considerable practical importance.

The significance of the attachment line with respect to laminar flow control has been recognized for many years (see Pfenninger (1977)). The previous work on this problem has been almost wholly experimental though, following Gregory, Stuart, and Walker (1955), there have been many theoretical investigations of crossflow instabilities which are important outside the attachement region. The small amplitude stability problem was first considered by Gaster (1967) who introduced controlled acoustic disturbances into the attachment line flow formed upon a faired circular cylinder model. From his measurements he concluded that the swept attachment line boundary layer was stable to small amplitude disturbances for momentum thickness Reynolds numbers up to at least 170. In a later investigation Cumpsty and Head (1969) reported that no instability was observed for R_θ up to 240. The first experimental investigation to detect amplified attachment line disturbances was conducted by Pfenninger and Bacon (1969). Their test configuration consisted of a 45° swept back wing with a blunt-nosed aerofoil section which also had provision for surface suction through closely spaced slots. The results of this experiment will be discussed in depth later in

this paper. More recently, an investigation of the stability characteristics of the attachment line flow on a swept cylinder has been carried out by Poll (1979 and 1980). In these tests, which were similar in some respects to those conducted by Pfenninger and Bacon, amplified disturbances were observed and recorded. By combining the results of all the available experimental data including the little known work of Carlson (1966), Poll argued that the upper limit for the stability of the laminar swept attachment line boundary layer flow occurs at a momentum thickness Reynolds number of approximately 230.

In this paper we investigate the instability of a three-dimensional boundary layer which is directly relevant to the experimental configurations of Pfenninger, Bacon and Poll. The relevance of the flow will be immediately obvious when we describe it but we postpone until the last section of this paper a more detailed discussion of the relationship between the experimental situation and our idealized model.

We consider the flow adjacent to the infinite flat plate defined by $y = 0$ with respect to Cartesian coordinates (x,y,z) with the x and z axes lying in the plate. The velocity components in the x and z directions are zero at the plate and approach the values $U_0 \frac{x}{\ell}$ and W_0 respectively when $y \to \infty$. The normal velocity component takes on the constant value V_0 at the wall and grows linearly with y when $y \to \infty$. The important simplifying feature of this flow is that it corresponds to an exact solution of the Navier-Stokes equations so that it is not necessary for us to make the boundary layer approximation when deriving the basic flow. Thus it is sensible for us to discuss the stability of the flow at finite Reynolds number and the concept of a critical Reynolds number is tenable. This is in contrast to the situation with Blasius flow where a self-consistent

perturbation investigation of the linear stability problem does not lead to a critical Reynolds number. The latter problem has been discussed by Smith (1979) and Bodonyi and Smith (1981).

The basic flow described above is susceptible to centrifugal instabilities because of the curvature of the streamlines in the x-y plane. In particular when $W_0 = 0$ the plane stagnation point stability equations of Hämmerlin (1955) are recovered when a disturbance periodic in z is imposed on the flow. Hämmerlin showed that a continuous spectrum of neutrally stable wavenumbers exists for these equations. The eigenfunctions corresponding to these modes decay algebraically with y but it is yet to be shown that they are physically relevant in a more realistic situation where they must be matched onto a disturbance outside the attachment region. There also exists a discrete spectrum of damped eigenvalues having eigenfunctions which decay exponentially when $y \to \infty$ and it is this type of eigenvalue on which we will concentrate our attention here.

If W_0 is nonzero the spanwise velocity component is susceptible to Tollmien-Schlichting waves but we show that there is no rational approximation which leads to the Orr-Sommerfeld eigenvalue problem. Instead we find that the appropriate eigenrelation is of sixth order in y and reduces to that obtained by Hämmerlin in the limit $W_0 \to 0$.

The numerical solution of the eigenvalue problem is nontrivial because of the rapidly varying nature of the eigenfunctions and two independent schemes were used in our calculations. The most efficient scheme was a fourth-order compact finite difference method based on that described by Malik, Chuang and Hussaini (1982). In addition the Riccati method was also used to provide a check on the eigenvalues obtained from the finite difference method.

Our calculations showed that at a critical value of W_0 the attachment line boundary layer is unstable to discrete Tollmien-Schlichting instabilities. Moreover, these modes are connected to the discrete modes of the plane stagnation point stability problem found by Wilson and Gladwell (1979) so that we have an additional check on the numerical work. The eigenfunctions associated with the discrete spectrum change from being of typical Taylor-Görtler type at small values of W_0 to being of Tollmien-Schlichting type when instability occurs.

The results which we obtain for the basic flow described previously can be applied to the experiments of Pfenninger and Bacon (1969) and Poll (1979,1980). We shall compare our predicted frequencies with those given by these authors and there seems to be little doubt that the instability mechanism which we investigate is responsible for that found experimentally.

The procedure adopted in the rest of this paper is as follows: in Section 2 we derive the basic flow and formulate the eigenvalue problem governing the stability of this flow to spanwise periodic disturbances. In Section 3 we discuss the boundary conditions at infinity which must be imposed before the eigenvalue problem can be solved. In Section 4 we discuss the numerical work required to calculate the basic flow and solve the eigenvalue problem. In Section 5 we discuss the asymptotic limit of large suction whilst in Section 6 we discuss the relevance of our results to experimental observations.

2. THE BASIC FLOW AND THE DISTURBANCE EQUATION

We consider the flow of a viscous incompressible fluid of kinematic viscosity ν adjacent to a flat plate defined by $y = 0$ with respect to the

Cartesian coordinate system (x,y,z). The y axis is taken to be normal to the wall and we look for a solution of the Navier-Stokes equations which satisfies the conditions

$$u = w = 0, \qquad v = V_0, \qquad y = 0,$$

$$(2.1)$$

$$u \to U_0 \frac{x}{\ell}, \qquad w \to W_0, \qquad y \to \infty,$$

where ℓ is a length scale in the x direction whilst U_0, V_0 and W_0 are independent velocity scales. We define the parameters Δ, R, and κ by

$$\Delta = \left(\frac{\nu\ell}{U_0}\right)^{1/2}, \qquad R = \frac{W_0 \Delta}{\nu}, \qquad \kappa = V_0\left(\frac{\ell}{\nu U_0}\right)^{1/2}. \qquad (2.2)$$

Thus, Δ is the thickness of the boundary layer associated with the flow in the x-y plane. It is known that there exists an exact solution of the Navier-Stokes equations corresponding to (2.1). The velocity field of this exact solution can be written

$$u = U_0 \frac{x}{\ell} \bar{u}(\eta), \qquad v = U_0 \frac{\Delta}{\ell} \bar{v}(\eta), \qquad w = W_0 \bar{w}(\eta), \qquad (2.3)$$

where

$$\eta = \frac{y}{\Delta} \qquad (2.4)$$

and $\bar{u}$, $\bar{v}$, $\bar{w}$ satisfy

$$\bar{u} + \bar{v}' = 0,$$

$$\bar{v}''' + \bar{v}'^2 - \bar{v}\,\bar{v}'' - 1 = 0, \qquad (2.5)$$

$$\bar{w}'' - \bar{v}\,\bar{w}' = 0,$$

$$\bar{v}'(0) = 0, \quad \bar{v}(0) = \kappa, \quad \bar{v}'(\infty) = -1, \quad \bar{w}(0) = 0, \quad \bar{w}(\infty) = 1.$$

We note that the solution of the above system has

$$v \sim -\left(\eta - \delta(\kappa)\right) \quad \text{when} \quad \eta \to \infty,$$

where the displacement $\delta(\kappa)$ is, of course, a function of κ. We further note that if $\kappa > 0$, then $\overline{w}''$ will necessarily vanish at some values of η so that if $\overline{u}$ and $\overline{v}$ are, in some sense, negligible in the stability calculation we expect inflection point instabilities to occur.

We restrict our attention to the linear stability of the flow (2.3) to disturbances periodic in the z-direction with wavelengths $\frac{2\pi\Delta}{\alpha}$. We shall take α to be real and look for the corresponding complex frequency associated with α for each value of R and κ. We perturb the flow (2.3) by writing

$$\frac{u}{W_0} = \frac{x}{\ell}\left[\varepsilon\overline{u} + \varepsilon RUE\right],$$

$$\frac{v}{W_0} = \frac{\overline{v}}{R} + VE, \qquad (2.6)$$

$$\frac{w}{W_0} = \overline{w} + WE,$$

where $\varepsilon = \dfrac{U_0}{W_0}$ and $E = \exp i\,\alpha\left\{\dfrac{z}{\Delta} - \dfrac{ctW_0}{\Delta}\right\}$. It will also be useful to work with the quantities ω, λ given by

$$\omega = \alpha c, \quad \lambda = -i\alpha Rc. \qquad (2.7)$$

The pressure perturbation corresponding to (U, V, W) is $\rho W_0^2 PE$ and U, V, W and P are functions of the nondimensional variable η defined by (2.4). The x-dependence of the disturbance which we have assumed corresponds

to that used by Hämmerlin (1955) and enables us to find a solution of the linear stability equations by solving ordinary differential equations. Such a simplification does not happen in more general boundary layer centrifugal instability problems and a self-consistent linear stability analysis leads to a partial differential system (see Hall (1983)). It is a routine matter to substitute the disturbed flow velocity and pressure fields into the Navier-Stokes equations and linearize in U, V, W to obtain:

$$\left\{\frac{d^2}{d\eta^2} - \alpha^2\right\}U = -i\alpha RcU + 2\overline{u}\,U + V\overline{u}' + \overline{v}U' + i\alpha R\overline{w}\,U, \tag{2.8a}$$

$$\left\{\frac{d^2}{d\eta^2} - \alpha^2\right\}V = RP' - i\alpha RcV + \overline{v}V' + \overline{v}'V + i\alpha R\overline{w}V, \tag{2.8b}$$

$$\left\{\frac{d^2}{d\eta^2} - \alpha^2\right\}W = i\alpha RP - i\alpha RcW + \overline{v}W' + RV\overline{w}' + i\alpha R\overline{w}W, \tag{2.8c}$$

$$U + V' + i\alpha W = 0. \tag{2.8d}$$

The pressure perturbation P and the z component of velocity W can be eliminated from (2.8) to give the following pair of coupled equations to determine U and V;

$$\left\{M + i\alpha Rc\right\}U = 2\overline{u}U + \overline{u}'V + \overline{v}U' + i\alpha R\overline{w}U, \tag{2.9a}$$

$$\left\{M + i\alpha Rc\right\}MV = i\alpha R\overline{w}MV - i\alpha R\overline{w}''V + \overline{v}MV' + \overline{v}'MV - 2\overline{u}'U - 2\overline{u}U' - \overline{u}''V - \overline{u}'V'. \tag{2.9b}$$

Here the operator M is defined by

$$M \equiv \frac{d^2}{d\eta^2} - \alpha^2,$$

and we see that (2.9) with $R = 0$ reduce to the usual equations governing the stability of stagnation point flow to Taylor-Görtler instabilities. Alternatively by setting $\overline{u} = \overline{v} = 0$ in (2.9b) we obtain the Orr-Sommerfeld equation for V. However, it is clear that there is no rational approximation to (2.9) which decouples the equations in order to produce the latter simplification. Before discussing the numerical solution of (2.9) we must derive the appropriate form of the disturbance for $\eta \gg 1$, this will enable us to generate boundary conditions at $\eta = \eta_\infty \gg 1$.

3. THE BOUNDARY CONDITIONS TO BE IMPOSED AT $\eta = \infty$ AND THE CONTINUOUS SPECTRUM

Suppose next that we let $\eta \to \infty$ in (2.9) and replace $\overline{u}, \overline{v}, \overline{w}$ by their asymptotic expansions for $\eta \gg 1$ to obtain

$$[M - \lambda - 2 - i\alpha R]U + [\eta - \delta]U^{\prime} = 0, \tag{3.1a}$$

$$[M - \lambda - i\alpha R]MV + [\eta - \delta]MV^{\prime} + MV + 2U^{\prime} = 0, \tag{3.1b}$$

where λ is given by (2.7). If we look for asymptotic solutions of (3.1) with U and V having an algebraic dependence on $[\eta - \delta]$ we obtain the two independent solutions

a. $U \sim (\eta^-)^{\lambda+2+i\alpha R+\alpha^2}$, $V \sim (\eta^-)^{\lambda+1+i\alpha R+\alpha^2}$,

b. $U = 0$, $V \sim (\eta^-)^{\lambda-1+i\alpha R+\alpha^2}$,

where $\eta^- = \eta - \delta$. In addition, there exist the following three independent exponentially decaying solutions:

c. $U = 0$, $V \sim e^{-\alpha\eta^-}$,

d. $U = 0$, $V \sim (\eta^-)^{-2-\alpha^2-\lambda-i\alpha R} e^{-\eta^{-2}/2}$,

e. $U \sim (\eta^-)^{-3-\alpha^2-\lambda-i\alpha R} e^{-\eta^{-2}/2}$, $V \sim \dfrac{[3 + \alpha^2 + \lambda + i\alpha R]}{2} \dfrac{U}{\eta^{-3}}$.

Suppose that λ is constrained to lie in the half plane $\lambda_r < -2 - \alpha^2$ and we impose the condition U, V, W $\to$ 0 when $\eta \to \infty$. We see that there are five independent solutions of (2.9) which have this property and they correspond to the asymptotic forms (a) - (e). Each of these solutions can be multiplied by an arbitrary constant, $\alpha_a, \cdots, \alpha_e$, and the solutions must then be combined so as to satisfy

$$U(0) = V(0) = V^-(0) = 0. \tag{3.2}$$

Thus for each $\lambda_r < -2 - \alpha^2$ there are two independent eigenfunctions corresponding to say, $\alpha_a = 0$ and $\alpha_b = 0$. We refer to these eigenfunctions as the B and A eigenfunctions respectively. We further note that the pressure perturbation corresponding to these eigenfunctions also tends to zero when $\eta \to \infty$.

Suppose next that λ_r is constrained to be in the interval $-2 - \alpha^2 < \lambda_r < 1 - \alpha^2$ so that (a) no longer gives algebraic decay for U when $\eta \to \infty$. However, the asymptotic form (b) still corresponds to algebraic decay of the disturbance when $\eta \to \infty$ so that there exists one eigenfunction (i.e., the B eigenfunction) corrersponding to each λ in this strip. In particular, if we set $\lambda = 0$, $R = 0$, we obtain the continuous spectrum $0 < \alpha < 1$ which was discussed by Hämmerlin (1955).

The eigenfunctions of the continuous spectra discussed above have the property that the velocity fields tend to zero algebraically when $\eta \to \infty$. If this condition is replaced by one which requires that U, V, W should tend to zero exponentially when $\eta \to \infty$, then only (c), (d), and (e) can be used to generate independent solutions of (2.9). In this case the three independent solutions of (2.9) must be combined to satisfy (3.2) and then only a discrete spectrum will exist. This possibility was investigated by Wilson and Gladwell (1978) who considered the plane stagnation point problem $R = 0$. The latter case is that discussed by Hämmerlin (1955) and Wilson and Gladwell found a damped discrete spectrum corresponding to disturbances which decay exponentially when $\eta \to \infty$. It was suggested by the latter authors that the continuous spectrum is not physically relevant for the reasons we discuss below.

Suppose that the basic flow which we are considering is the local flow near the attachment line on, say, an infinitely long swept cylinder. The disturbances which we are calculating must then be matched with a disturbed flow in the appropriate ´outer region´ unless they decay exponentially when $\eta \to \infty$, in which case the disturbed flow is confined to the boundary layer. Thus the physical relevance of the continuous spectrum in this more realistic

flow is not known until the disturbance flow field in the ´outer region´ has been found. It seems that, as yet, the latter structure has not been determined so that the relevance of the continuous spectrum remains an open question. Wilson and Gladwell argue that the algebraic decay of the continuous spectrum eigenfunctions will lead to inconsistencies in the matching procedure between the inner and outer region. This is indeed possible but perhaps a more likely outcome is that only the unstable part of the continuous spectrum would be ruled out by such a procedure. Without solving the outer problem the above arguments are merely speculative but it is clear that the exponential decay of the discrete spectrum removes any doubt about its relevance to more realistic flows. For that reason we shall confine our attention to the discrete spectrum but we must bear in mind that the continuous spectrum may play an important role the linear stability problem under investigation. Indeed, Dhanak and Stuart[1] who investigated the problem with $R = 0$, argue that even some of the algebraically growing solutions of (2.9) are physically relevant. However, the close agreement between experimental observations and our results suggests that the discrete modes with exponential decay at infinity dominate the boundary layer stabilty characteristics on a swept cylinder. Finally, we note that if U and V are to decay exponentially when $\eta \to \infty$ then for sufficiently large values of η, $U \sim e^{-\eta^2/2}$, $V \sim e^{-\alpha\eta}$. Thus the normal velocity component V decays to zero more slowly than U.

---

[1]M. Dhanak and J. T. Stuart, 1983, Imperial College, England, personal communication, to be published.

4. THE NUMERICAL WORK

The first step in the calculations was to integrate (2.5) by a shooting method by guessing an initial value for $\bar{v}''(0)$ and iterating until $\bar{v}'(\infty) = -1$. The results obtained were in excellent agreement with those given in Rosenhead (1963).

The linear stability equations (2.9) were then integrated subject to (3.2) together with the condition that (U, V, W) should tend exponentially to zero when $\eta \to \infty$. The first method used was a shooting procedure which though able to reproduce Wilson and Gladwell's results at $R = 0$ without much difficulty or expense proved prohibitively expensive at higher values of the Reynolds number where instability is possible. For that reason the following independent schemes were implemented.

I. The Riccati Transform Method

A detailed account of this method can be found in, for example, Aziz (1973), Scott (1973), Davey (1977) or Sloan (1977). Davey (1977) has compared the efficiency of the method to an orthonormalization method for Orr-Sommerfeld equations whilst Wilson and Gladwell (1978) used the method for the plane stagnation point problem. The system (2.9) is written in the form

$$\frac{d\underline{y}_1}{d\eta} = A_1 \, \underline{y}_1 + A_2 \, \underline{y}_2, \tag{4.1a}$$

$$\frac{d\underline{y}_2}{d\eta} = A_3 \, \underline{y}_1 + A_4 \, \underline{y}_2, \tag{4.1b}$$

where A_1, A_2, A_3 and A_4 are defined by

$$A_1 = \begin{bmatrix} 0 & 0 & 0 \\ 0 & 0 & 1 \\ 0 & 0 & 0 \end{bmatrix}, \qquad A_2 = \begin{bmatrix} 1 & 0 & 0 \\ 0 & 0 & 0 \\ 0 & 1 & 0 \end{bmatrix},$$

$$A_3 = \begin{bmatrix} \alpha^2 + \lambda + 2\bar{u} + i\alpha\bar{R}\bar{w} & \bar{u}' & 0 \\ 0 & 0 & 0 \\ -2\bar{u}' & -\{\alpha^4 + \alpha^2\lambda + i\alpha^3 \bar{R}\bar{w}'' + \alpha^2 \bar{v}' + \bar{u}''\} & -\alpha^2 \bar{v} - \bar{u}' \end{bmatrix},$$

$$A_4 = \begin{bmatrix} \bar{v} & 0 & 0 \\ 0 & 0 & 1 \\ -2\bar{u} & 2\alpha^2 + \lambda + \bar{v} + i\alpha\bar{R}\bar{w} & \bar{v} \end{bmatrix},$$

and

$$\underline{y}_1 = (U,V,V')^T, \quad \underline{y}_2 = (U',V'', V''').$$

The matrix T, defined by $\underline{y}_2 = T\,\underline{y}_1$, satisfies the equation

$$\frac{dT}{d\eta} = A_1 T - TA_4 + A_2 - TA_3 T, \qquad (4.2)$$

whilst $S = T^{-1}$ satisfies

$$\frac{dS}{d\eta} = A_4 S - SA_1 + A_3 - SA_2 S. \qquad (4.3)$$

Apart from the definition of $\underline{y}_1$ and $\underline{y}_2$ the above formulation follows closely that given by Wilson and Gladwell. The no-slip condition requires that T satisfies the initial condition

$$T(0) = 0, \qquad\qquad (4.4)$$

and (4.2) was then integrated from $\eta = 0$ to $\eta = \bar{\eta}$ using a fourth-order Runge-Kutta scheme. If $\bar{\eta}$ is taken to be large the matrix T contains exponentially large-elements so it is convenient to take $\bar{\eta} = 1$ and calculate S before integrating (4.3) from $\eta = \bar{\eta}$ to $\eta = \eta_\infty \gg 1$.

The three asymptotic forms (c), (d), and (e) found in Section 3 show that at large values of η

$$\underline{y}_1 = M_1 \begin{pmatrix} \alpha_c \\ \alpha_d \\ \alpha_e \end{pmatrix} , \qquad\qquad \underline{y}_2 = M_2 \begin{pmatrix} \alpha_c \\ \alpha_d \\ \alpha_e \end{pmatrix} ,$$

where M_1, M_2 are 3×3 matrices. Thus at $\eta = \eta_\infty$, we require that

$$SM_1 \begin{pmatrix} \alpha_c \\ \alpha_d \\ \alpha_e \end{pmatrix} = M_2 \begin{pmatrix} \alpha_c \\ \alpha_d \\ \alpha_e \end{pmatrix} ,$$

and the eigenvalue $\lambda = \lambda(\alpha, R, \kappa)$ can be found by iterating to make $\det(SM_1 - M_2) = 0$.

The step length of the Runge-Kutta integration and η_∞ were varied until λ was obtained with sufficient accuracy. We now describe an alternative method which was used to solve the eigenvalue problem.

II. A Compact Fourth-Order Finite Difference Scheme

The scheme which we now describe was proposed by Malik, Chuang and Hussaini (1982) and is derived by means of the Euler-Maclaurin formula:

$$\psi^k - \psi^{k-1} = \frac{h_k}{2} \left(\frac{d\psi^k}{d\eta} + \frac{d\psi^{k-1}}{d\eta} \right) - \frac{h_k^2}{12} \left(\frac{d^2 \psi^k}{d\eta^2} - \frac{d^2 \psi^{k-1}}{d\eta^2} \right) + 0(h_k^5), \quad (4.5)$$

where

$$\psi^k = \Psi(\eta_k) \quad \text{and} \quad h_k = \eta_k - \eta_{k-1}.$$

The nodes are distributed to resolve singular layers so that

$$\eta_k = L(k-1)/\left(Ng - (k-1) \right), \quad k = 1,2,\cdots,N + 1, \quad (4.6)$$

where $N + 1$ is the total number of nodes, $g = (\eta_\infty + L)/\eta_\infty$, η_∞ the location of the boundary layer edge, and L a scaling parameter. We chose L to be twice the height (from the wall) of the nodal point at which the nondimensional mean velocity $\overline{w}$ assumed the value 0.5. It was found that for a given number of points, this choice of L in the grid distribution function (4.6), yielded maximum accuracy.

In order to apply the above compact difference scheme to (2.9a,b), it is necessary to write them as a set of first-order differential equations. They are rewritten as

$$\frac{d\phi_i}{d\eta} = \sum_{j=1}^{6} a_{ij} \phi_j; \quad i = 1,2,\cdots,6, \quad (4.7)$$

where

$$\phi_1 = v, \qquad \phi_2 = \frac{d\phi_1}{d\eta},$$

$$\phi_3 = \frac{d\phi_2}{d\eta}, \qquad \phi_4 = \frac{d\phi_3}{d\eta},$$

$$\phi_5 = U, \qquad \phi_6 = \frac{d\phi_5}{d\eta},$$

with the boundary conditions

$$\phi_1 = \phi_2 = \phi_5 = 0 \qquad\qquad\qquad\qquad \text{at} \quad \eta = 0, \qquad (4.8)$$

$$\phi_2 + \alpha\phi_1 = \phi_3 + \alpha\phi_2 = \phi_6 + \eta\phi_5 = 0, \qquad \eta = \eta_\infty. \qquad (4.9)$$

The latter conditions follow from the discussion of Section 3 where it was shown that for sufficiently large values of η

$$U \sim e^{-\eta^2/2}, \qquad V \sim e^{-\alpha\eta}.$$

The nonzero elements of the matrix (a_{ij}) are

$$a_{12} = 1,$$

$$a_{23} = 1,$$

$$a_{34} = 1,$$

$$a_{41} = -\alpha^4 + i\alpha^2 \omega R - i\alpha^3 R\overline{w} - \alpha^2 \overline{v} - i\alpha R \overline{w}'' - \overline{u}'',$$

$$a_{42} = -\alpha^2 \bar{v} - \bar{u}',$$

$$a_{43} = 2\alpha^2 - i\omega R + i\alpha R\bar{w} + \bar{v}',$$

$$a_{44} = \bar{v},$$

$$a_{45} = -2\bar{u}',$$

$$a_{46} = -2\bar{u},$$

$$a_{65} = \alpha^2 - i\omega R + 2\bar{u} + i\alpha R\bar{w},$$

$$a_{66} = \bar{v}.$$

We set

$$\Psi = \{\phi_i\}, \quad \frac{d\Psi}{d\eta} = \left\{ \sum_{j=1}^{6} a_{ij} \phi_j \right\}, \quad \frac{d^2\Psi}{d\eta^2} = \left\{ \sum_{j=1}^{6} b_{ij} \phi_j \right\},$$

where

$$b_{ij} = \frac{da_{ij}}{d\eta} + \sum_{\ell=1}^{6} a_{i\ell} a_{\ell j}$$

and thus (4.5) becomes

$$\phi_i^k - \frac{h_k}{2} \sum_{j=1}^{6} a_{ij}^k \phi_j^k + \frac{h_k^2}{12} \sum_{j=1}^{6} b_{ij}^k \phi_j^k$$

$$- \left\{ \phi_i^{k-1} + \frac{h_k}{2} \sum_{j=1}^{6} a_{ij}^{k-1} \phi_j^{k-1} + \frac{h_k^2}{12} \sum_{j=1}^{6} b_{ij}^{k-1} \phi_j^{k-1} \right\} = 0, \quad (4.10)$$

$$k = 2, 3, \cdots, N + 1.$$

It is possible to write the above equation system along with the boundary conditions (4.8) − (4.9) in block-tridiagonal form:

$$A_k \, \phi^{k-1} + B_k \, \phi^k + C_k \, \phi^{k+1} = H, \quad k = 1,2,\cdots,N + 1 \qquad (4.11)$$

where A_k, B_k, C_k are 6×6 matrices defined below and H is a 6×1 null matrix.

$$
A_k = \left[\begin{array}{c} \text{Nonzero elements} \\ \hline 0 \end{array}\right] \begin{array}{l} 3 \text{ rows} \\ 3 \text{ rows} \end{array} \; ; \quad k = 2,\cdots,N + 1, \qquad (4.12)
$$

(6 columns)

$$
C_k = \left[\begin{array}{c} 0 \\ \hline \text{Nonzero elements} \end{array}\right] \begin{array}{l} 3 \text{ rows} \\ 3 \text{ rows} \end{array} \; ; \quad k = 1,\cdots,N. \qquad (4.13)
$$

(6 columns)

B_k are full matrices with $k = 1$ and $k = N + 1$ having the structure

$$
B_1 = \left[\begin{array}{c} E \\ \hline \text{Nonzero elements} \end{array}\right] \begin{array}{l} 3 \text{ rows} \\ 3 \text{ rows} \end{array} \qquad (4.14)
$$

(6 columns)

6 columns

$$B_{N+1} = \left[\begin{array}{c} \text{Nonzero elements} \\ \hline F \end{array}\right] \begin{array}{c} 3 \text{ rows} \\ 3 \text{ rows} \end{array} \qquad (4.15)$$

where E and F are 3×6 matrices representing the bottom and top boundary conditions (4.8) and (4.9) respectively. Thus we obtain

$$E = \begin{bmatrix} 1 & 0 & 0 & 0 & 0 & 0 \\ 0 & 1 & 0 & 0 & 0 & 0 \\ 0 & 0 & 0 & 0 & 1 & 0 \end{bmatrix} \qquad (4.16)$$

and

$$F = \begin{bmatrix} \alpha & 1 & 0 & 0 & 0 & 0 \\ 0 & \alpha & 1 & 0 & 0 & 0 \\ 0 & 0 & 0 & 0 & \eta & 1 \end{bmatrix} . \qquad (4.17)$$

We can write (4.11) in the form

$$\mathcal{L}\phi = H \qquad (4.18)$$

where $\mathcal{L} = [A_k, B_k, C_k]$.

Assuming an estimate of the eigenvalue is available, we solve (4.18) directly. In order to avoid the trivial solution, nonhomogeneous boundary conditions are imposed at the wall. Specifically, the boundary condition $\phi_1(0) = 0$ is replaced by $\phi_3(0) = 1$. This is equivalent to normalizing the eigensolution by the value of $\dfrac{d^2 V}{d\eta^2}$ at the wall. Matrix E of (4.16) now becomes

$$E = \begin{bmatrix} 0 & 0 & 1 & 0 & 0 & 0 \\ 0 & 1 & 0 & 0 & 0 & 0 \\ 0 & 0 & 0 & 0 & 1 & 0 \end{bmatrix}$$

and

$$H = (1, \ 0, \ 0, \cdots, 0)^T.$$

The system (4.18) is nonhomogeneous and the nontrivial solution is obtained using block LU factorization. Newton's method is then used to iterate on the eigenvalue such that the remaining boundary condition $\phi_1(0) = 0$ is satisfied.

In order to generate neutral curve $(\omega_i = 0)$, a solution ϕ is first obtained for assumed values of α and ω_r. The corrections $\Delta\alpha$ and $\Delta\omega_r$ are then determined from the equations:

$$\phi_{1_r}(0) + \frac{\partial\phi_{1_r}(0)}{\partial\alpha}\Delta\alpha + \frac{\partial\phi_{1_r}(0)}{\partial\omega_r}\Delta\omega_r = 0, \qquad (4.19a)$$

$$\phi_{1_i}(0) + \frac{\partial\phi_{1_i}(0)}{\partial\alpha}\Delta\alpha + \frac{\partial\phi_{1_i}(0)}{\partial\omega_r}\Delta\omega_r = 0. \qquad (4.19b)$$

Here $\phi_1(0)$ is known from the solution ϕ just obtained whilst the derivatives with respect to α and ω_r are obtained by solving

$$\mathcal{L}\frac{\partial\phi}{\partial\alpha} = -\frac{\partial\mathcal{L}}{\partial\alpha}\phi \qquad (4.20)$$

and

$$\mathcal{L}\frac{\partial\phi}{\partial\omega_r} = -\frac{\partial\mathcal{L}}{\partial\omega_r}\phi. \qquad (4.21)$$

The process is repeated until $\phi_1(0)$ vanishes within preassigned tolerances. We see that (4.18), (4.20) and (4.21) can be solved with the same LU factorizations and both the eigenvalue and eigenfunction are obtained.

The two schemes described above were first used to calculate the eigenvalues of (2.9) with $R = 0$. The results obtained were found to be consistent with those given by Wilson and Gladwell (1978). At higher values of R, where instability is possible, the Riccati method gave consistent results provided that enough grid points were used. For Reynolds numbers less than ~ 1000 it was found necessary to use at least five hundred steps (with $\eta_\infty = 10$) to obtain a neutral eigenvalue correct to four significant figures. In Table I we have illustrated the convergence of the finite difference scheme in this region.

The convergence of the latter scheme is significantly faster than that of the Riccati method and the neutral values of α, c_r correct to four significant figures can be obtained with only forty-one grid points. Moreover, it was found that the iteration to an eigenvalue with the Riccati method was much more sensitive to the initial guess for the eigenvalue than was the case with the finite difference scheme. In view of the fact that the eigenfunctions cannot be calculated directly using the Riccati method because of numerical instabilities it was therefore decided to use the finite difference scheme to generate the neutral curves and use the Riccati method to check selected eigenvalues.

In Figure 1 we have shown the neutral wavenumber and frequency $\omega = \alpha c_r$ as functions of the Reynolds number R for $\kappa = -.8, -.4, 0, .1$. The critical values corresponding to the zero suction case $\kappa = 0$ are

$$R = 583.1, \qquad \alpha = .288, \qquad \alpha c_r = .111.$$

It is clear from Figure 1 that suction and blowing have stabilizing and destabilizing effects on the flow respectively. The shape of the neutral curves for $\kappa < 0$ is typical of viscous instabilities of flows without inflection points whereas the open neutral curves for $\kappa > 0$ are to be expected since $\bar{w}$ has an inflection point in this case. It should be noted that, although (2.9) is not the Orr-Sommerfeld equation, the inviscid limit of (2.9) is the Rayleigh equation so that in the absence of an inflection point the flow is stable at infinite Reynolds numbers.

In Figure 2 we have shown some of the eigenfunctions corresponding to the neutral curves of Figure 1. The eigenfunctions have been normalized in each case such that the maximum magnitude of each velocity component is unity. It can be seen that the x-velocity component goes to zero more quickly than the other two components. This is, of course, to be expected since we have shown earlier that for large η, $U \sim e^{-\eta^2/2}$ whilst the other velocity components go to zero like $e^{-\alpha\eta}$. We also notice that for the cases with $\kappa > 0$ the eigenfunctions have their critical layers further away from the wall than is the case with $\kappa < 0$.

In Figure 3 have have plotted the critical Reynolds numbers corresponding to $\kappa = +.8, +.4, 0, -.1, -.15, -.2$. We note that $\frac{V_0}{W_0} = \frac{\kappa}{R}$ so that the significant rise in the critical Reynolds number corresponding to $\kappa = -.1$ corresponds to $\frac{V_0}{W_0} \sim 10^{-4}$ which is well within the range of practical feasibility. Figure 3 suggests that the critical Reynolds number can be made arbitrarily large by taking $-\kappa \ll 1$. In order to determine whether this is the case we shall in the next section consider the structure of the neutral curve in the limit $\kappa \to -\infty$.

5. THE LARGE SUCTION LIMIT $\kappa \to -\infty$

We first consider the limiting form of the solution of (2.5) when $\kappa \to -\infty$. For $\eta \sim 0(1)$, it is easily shown that the asymptotic form of $\overline{v}$ is

$$\overline{v} \sim \kappa - \frac{\eta^2}{2\kappa} + \cdots \quad , \tag{5.1a}$$

whilst

$$\overline{u} \sim \frac{\eta}{\kappa} + \cdots \quad , \tag{5.1b}$$

It follows from the z momentum equation that $\overline{w}$ then approaches unity on the length scale $|\kappa|^{-1}$ so that if we write

$$\xi = \eta |\kappa|$$

then for $\xi \sim 0(1)$

$$u \sim \frac{-\xi}{\kappa^2} + \cdots, \quad \overline{v} \sim \kappa \frac{-\xi}{2\kappa^3} + \cdots, \quad \overline{w} = (1 - e^{-\xi}) + \cdots \quad . \tag{5.2}$$

Thus $\overline{w}$ is given to first order by the asymptotic suction velocity profile and before determining the corresponding asymptotic structure of U, V we first write

$$\alpha = |\kappa| a, \tag{5.3a}$$

$$R = |\kappa| \tilde{R}. \tag{5.3b}$$

The above rescaling is suggested by the fact that the appropriate length scaled for the instability is now ν/V_0 and not Δ. It now remains for us

to rewrite (2.9) in terms of ξ and expand U, V in the form

$$U = \frac{U_0}{\kappa^3} + \frac{U_1}{\kappa^4} + \cdots$$

$$V = V_0 + \frac{V_1}{\kappa} + \cdots,$$

where U_0, V_1, etc. are functions only of ξ. It is then a routine matter to substitute the above expansions into (2.9) and determine U_0, V_0, etc. We find that V_0 satisfied the equation

$$\left\{\frac{d^2}{d\xi^2} - a^2 + ia\tilde{R}c\right\}\left\{\frac{d^2}{d\xi^2} - a^2\right\}V_0 = ia\tilde{R}[1-e^{-\xi}]V_0 + ia\tilde{R}e^{-\xi}V_0 - \left\{\frac{d^3}{d\xi^3} - a^2\frac{d}{d\xi}\right\}V_0.$$

(5.4)

which is just the modified Orr-Sommerfeld equation for the asymptotic suction profile. The appropriate boundary conditions for (5.4) are

$$V_0 = V_0' = 0, \quad \xi = 0, \quad V_0 \to 0, \quad \xi \to \infty. \tag{5.5}$$

There is no continuous spectrum of (5.4) corresponding to (5.5) and the critical Reynolds number associated with the discrete spectrum is given by Hocking (1974) as

$$\tilde{R} = 54,370$$

whilst the critical values of a, c are

$$a = .1555, \quad c = .150.$$

Hence, we see that in the limit of large suction (2.9) simplifies to the modified Orr-Sommerfeld equation for the asymptotic suction profile and the critical value of R is given asymptotically by

$$R \sim 54,370 \, |\kappa|. \tag{5.6}$$

The massive stabilizing effect of suction suggested by Figure 3 is therefore not surprising. It follows from (5.6) that R can be made arbitrarily large by taking the limit $\kappa \rightarrow -\infty$ but that instability then always occurs when $\dfrac{V_0}{W_0} = \dfrac{1}{54,370}$ and is confined to a layer of thickness (ν/V_0) at the wall.

6. DISCUSSION

We have shown that the attachment line boundary layer flow (2.3) is susceptible to travelling wave instabilities which propagate along the attachment line. These disturbances decay exponentially at the edge of the boundary layer and at zero Reynolds number correspond to the eigenvalues of the plane stagnation point stability problem found by Wilson and Gladwell (1979). The exponential decay of the eigenfunctions ensures that in more realistic situations there will be no difficulty matching the solutions onto the appropriate outer flow field. We now turn to the relevance of our work to the available experimental results which correspond to the flows around swept flat-nosed wings and circular cylinders. Before doing so, it is of course necessry to indicate the relevance of our basic flow to these

configurations. A discussion of the boundary layer flow on an infinitely long swept cylinder is given in Chapter VII of Rosenhead (1963) and is based on the work of Schubart (1945, unpublished), and Sears (1948, 1952).

The procedure is essentially identical to that appropriate to the two-dimensional case and outside the boundary layer the basic flow is expanded in the form

$$u = U_0 \frac{x}{\ell} + U_1\left(\frac{x}{\ell}\right)^3 + \cdots,$$

$$w = W_0 + \cdots \quad.$$

In the boundary layer the velocity components are expanded in powers of $\frac{x}{\ell}$ and the first order flow is exactly that which we have described in Section 2. Thus, sufficiently close to the attachment line, the basic flow which we have calculated in Section 2 gives a good approximation to the attachment line boundary layer on a swept cylinder. The range of validity of our theory will therefore depend on the cross-sectional shape of the cylinder and the Reynolds number.

The experimental investigations most relevant to the present work are due to Gaster (1967), Pfenninger and Bacon (1969) and Poll (1979, 1980). The first two investigations were concerned with the attachment lines on swept wings whilst Poll performed experiments on a swept circular cylinder. However, the wing section used by Pfenninger and Bacon had a flat nose so it is likely that our theoretical work is most relevant to their experiments. It is well-known that the attachment line is turbulent when large amplitude disturbances are present. These large amplitude disturbances convected into the attachment line can be prevented by various means so that the linear

critical Reynolds number almost certainly gives an upper limit to the laminar flow regime. Gaster found that the attachment line boundary layer is stable up to $R \sim 420$ which was the maximum value of the Reynolds number which could be achieved experimentally.

Pfenninger and Bacon (1969) and Poll (1979, 1980) measured equilibrium frequencies of naturally occuring small disturbances at various values of the Reynolds number. We have indicated these experimental results in Figure 4 where we have also shown the neutral curves without suction. The experimental points lie close to the lower branch of the neutral curve and the critical Reynolds number is close to the minimum Reynolds number at which Pfenninger and Bacon measured small amplitude equilibrium disturbances. It can be seen in Figure 7 of Pfenninger and Bacon (1969) that by introducing large amplitude disturbances into the boundary layer by means of trip wires it is possible to induce equilibrium disturbances at significantly lower values of the Reynolds number. The latter authors also give experimental points in the presence of suction but it is not clear from the results given whether the flow was stabilized or destabilized by the suction. The amount of suction used experimentally is not given by Pfenninger and Bacon but, in view of the results shown in Figure 3 of this paper, we assume that it was extremely small.

It seems likely that the instability mechanism which we have discussed is responsible for the disturbances measured experimetnally. Some further evidence for the relevance of our model is provided by Figure 5 which is taken from Poll (1980). Poll used two hot wires at the same spanwise location but different chordwise locations to measure the time history of the spanwise disturbance velocity component. The figure suggests that the instability is

indeed two-dimensional and takes the form of a time-harmonic disturbance propagating along the attachment line.

Finally we close by making a few comments about the extension of our analysis to include the effect of nonlinearity. Surprisingly, the disturbance structure (2.6) can still be retained and enables us to take out the x-dependence of the problem even in the nonlinear regime. Thus it is possible in principle to calculate the weakly nonlinear development of the disturbances considered in this paper. Such a calculation might explain the origin of the subcritical equilibrium disturbances measured by Pfenninger and Bacon (1969).

REFERENCES

[1] Aziz, A. K. (ed.), 1973, <u>Numerical Solution of Boundary Value Problems in Ordinary Differential Equations</u>, Academic Press.

[2] Bodonyi, R. J. and Smith, F. T., 1981, Proc. Roy. Soc. (A), <u>375</u>, 65.

[3] Carlson, J. C., 1966, Northrop Report, NOR-66-58.

[4] Cumpsty, N. A. and Head, M. R., 1969, The Aeronautical Quarterly, <u>20</u>, 99.

[5] Davey, A., 1977, J. Comput. Phys., <u>24</u>, 331.

[6] Gaster, M., 1967, The Aeronautical Quarterly, <u>18</u>, 165.

[7] Hall, P., 1983, J. Fluid. Mech., <u>130</u>, 41.

[8] Gregory, N., Stuart, J. T. and Walker, W. S., 1955, Phil. Trans. (A), <u>248</u>, 155.

[9] Hämmerlin, G., 1955, <u>50 Jahre Grenzschicht-forschung</u> (ed. H. Görtler, W. Tollmien) p. 304.

[10] Hocking, L. M., 1974, Quart. J. Mech. Appl. Math., <u>28</u>, 341.

[11] Malik, M. R., Chuang, S. and Hussaini, M. Y., 1982, ZAMP, <u>33</u>, 189.

[12] Pfenninger, W., 1977, AGARD Report 654.

[13] Pfenninger, W. and Bacon, J. W., 1969 <u>Viscous Drag Reduction</u>, C. S. Wells (ed.), Plenum Press, pp. 85-105.

[14] Poll, D. I. A., 1979, The Aeronautical Quarterly, <u>30</u>, 607.

[15] Poll, D. I. A., 1980, IUTAM Symposium on Laminar-Turbulent Transition, Stuttgart, Springer-Verlag.

[16] Rosenhead, L. (ed.), 1963, <u>Laminar Boundary Layers</u>, Oxford University Press.

[17] Scott, M. R., 1973, <u>Invariant Imbedding and its Application to Ordinary Differential Equations</u>, Addison-Wesley.

[18] Sears, W. R., 1948, J. Aeronautical Science, <u>15</u>, 49.

[19] Sloan, D. M., 1977, J. Comput. Phys., <u>24</u>, 320.

[20] Smith, F. T., 1979, Proc. Roy. Soc. (A), <u>366</u>, 91.

[21] Wilson, S. D. R. and Gladwell, I., 1978, J. Fluid Mech., <u>84</u>, 517.

Table I. The neutral eigenvalues as a function of the number of grid points of the finite difference scheme for R = 800, κ = 0.

10	.3300581	.1226919
20	.3378719	.1267951
40	.3384238	.1270776
80	.3384613	.1270965
160	.3384638	.1270977

Figure Captions

Figure 1a:

The neutral curves in the $\alpha - R$ plane for different values of κ.

Figure 1b:

The neutral curves in the $\omega - R$ plane for different values of κ.

Figure 2:

The neutral eigenfunctions for: (a) $R = 583.4$, $\alpha = 28$,

(b) $R = 4000$, $\alpha = .286$, (c) $R = 44.$, $\alpha = .4014$, (d) $R = 119$,

$\alpha = .3587$, (e) $R = 979$, $\alpha = .285$.

Figure 3:

The dependence of the critical Reynolds number on the suction parameters.

Figure 4:

A comparison between theory and experiment for $\kappa = 0$.

Figure 5:

The spanwise disturbance velocity components measured by Poll (1980) at neighbouring values of x with z fixed.
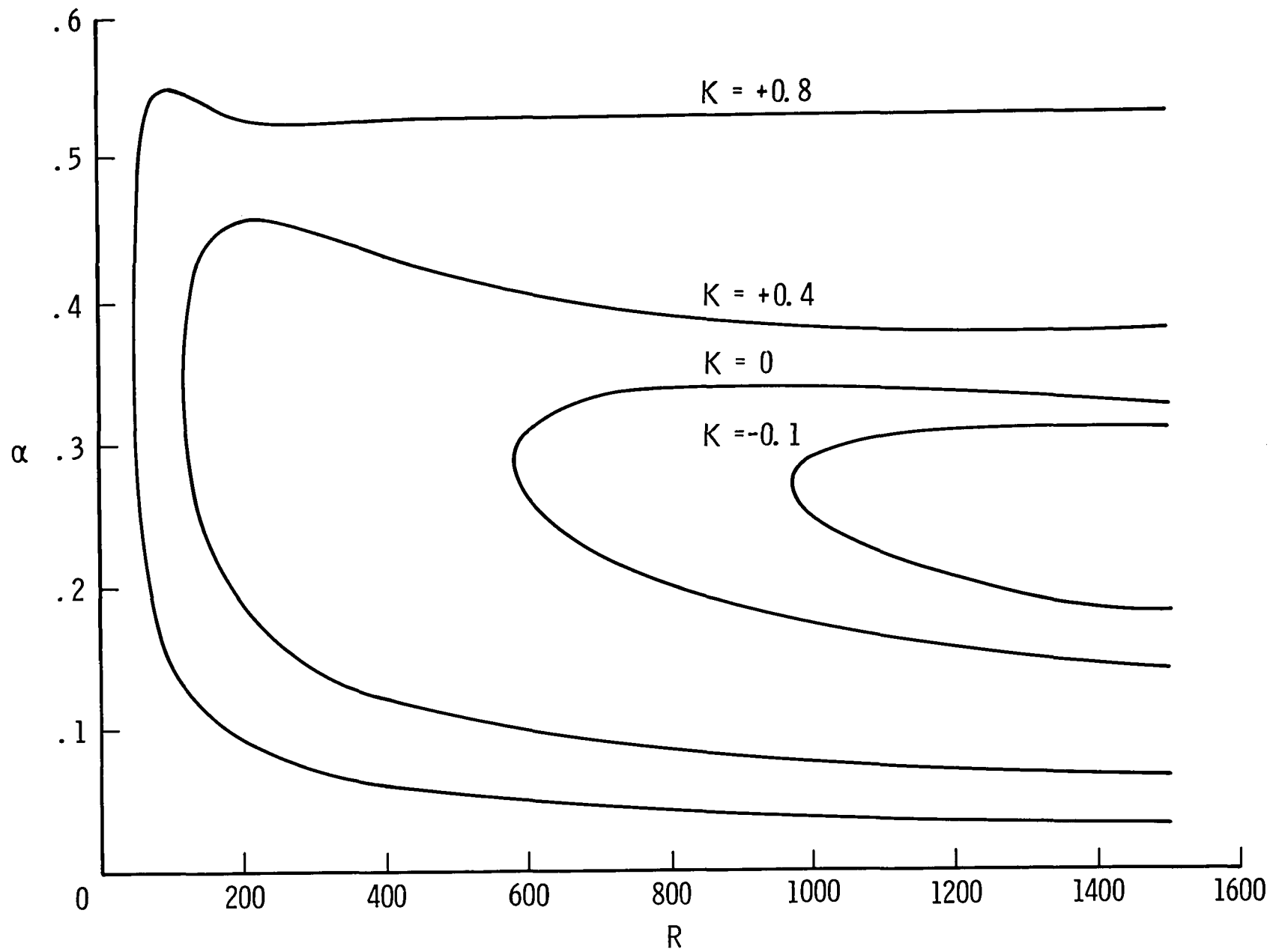
Figure 1a
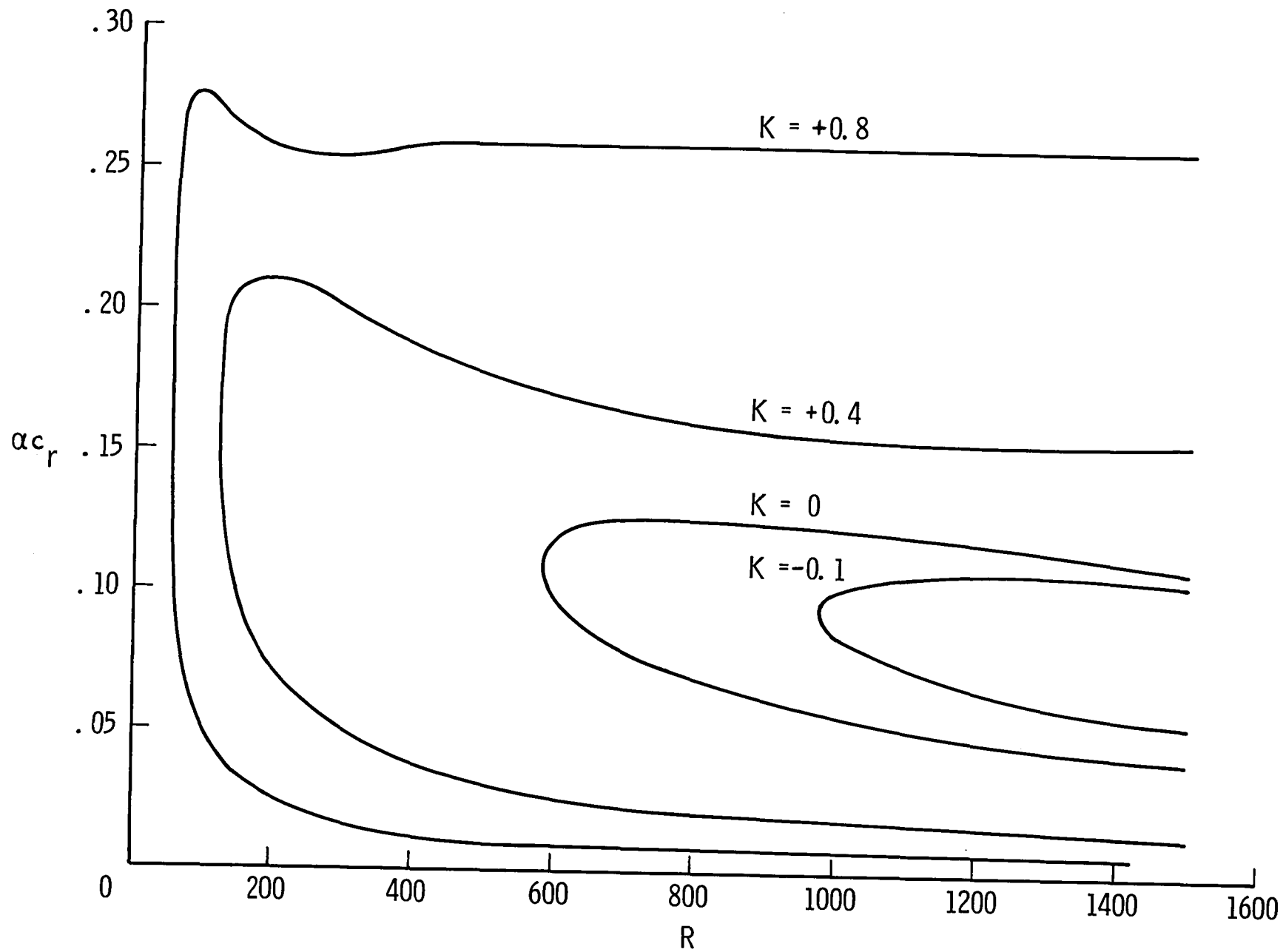
Figure 1b

Figure 2a
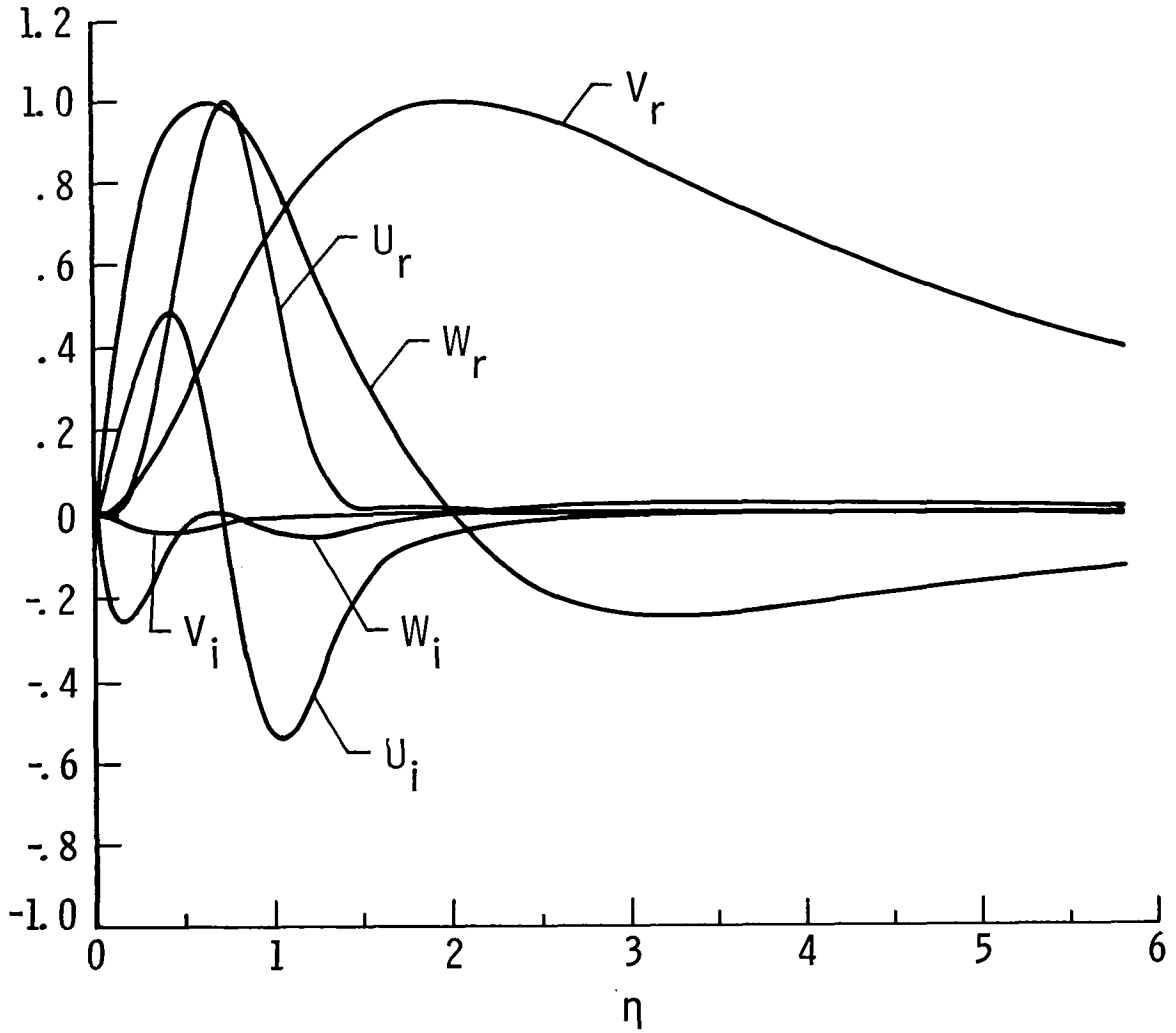
Figure 2b
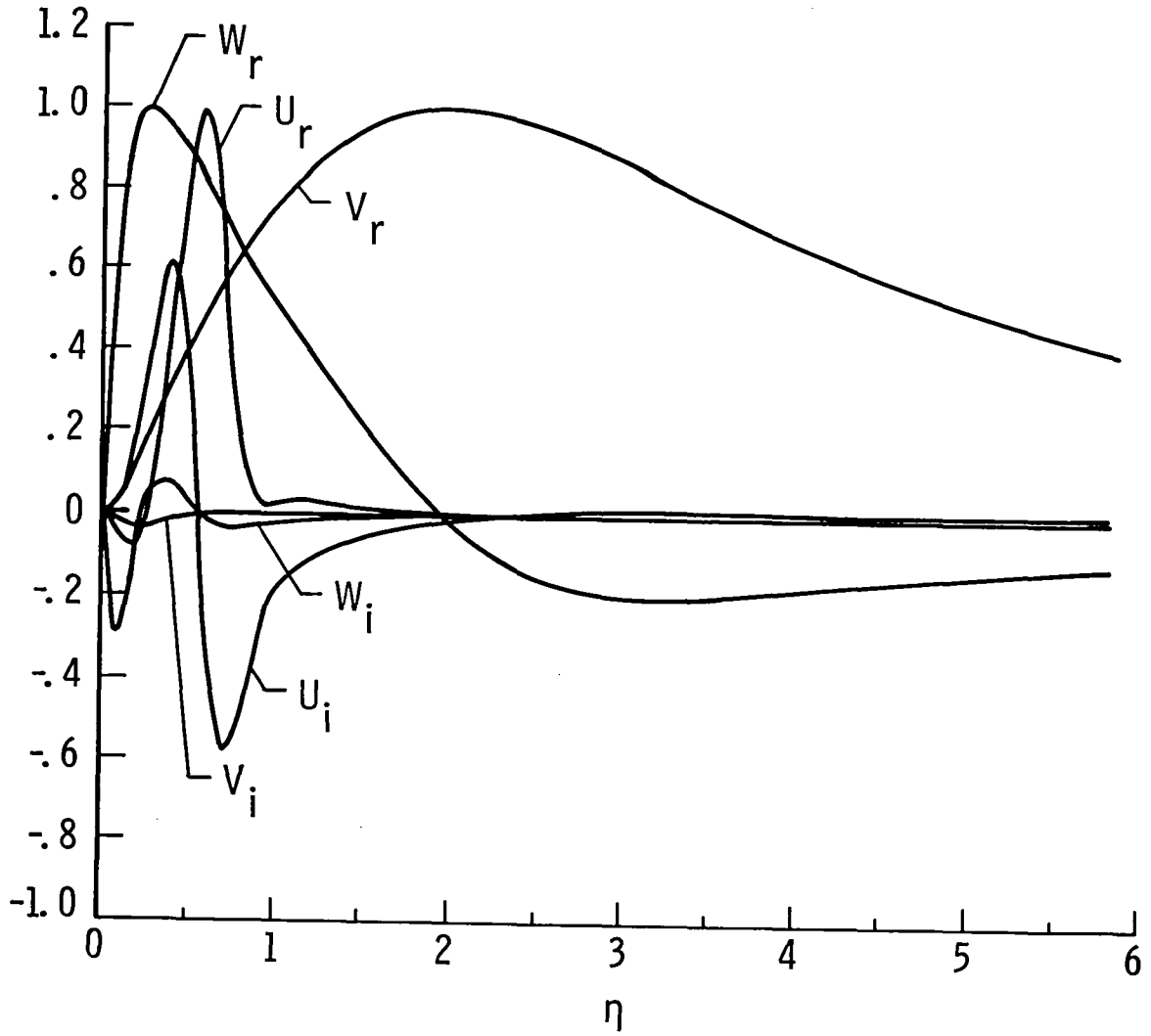
Figure 2c
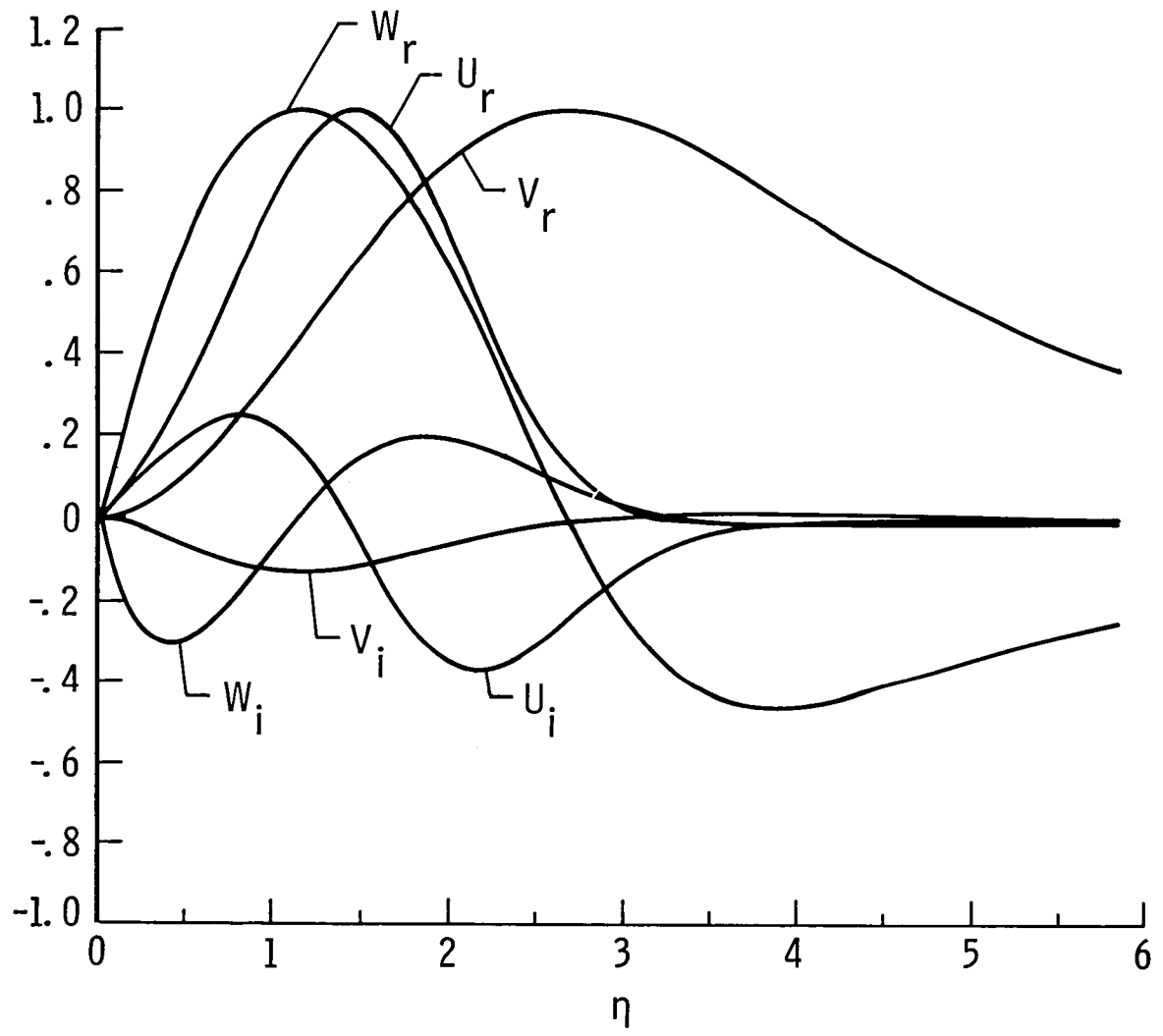
Figure 2d
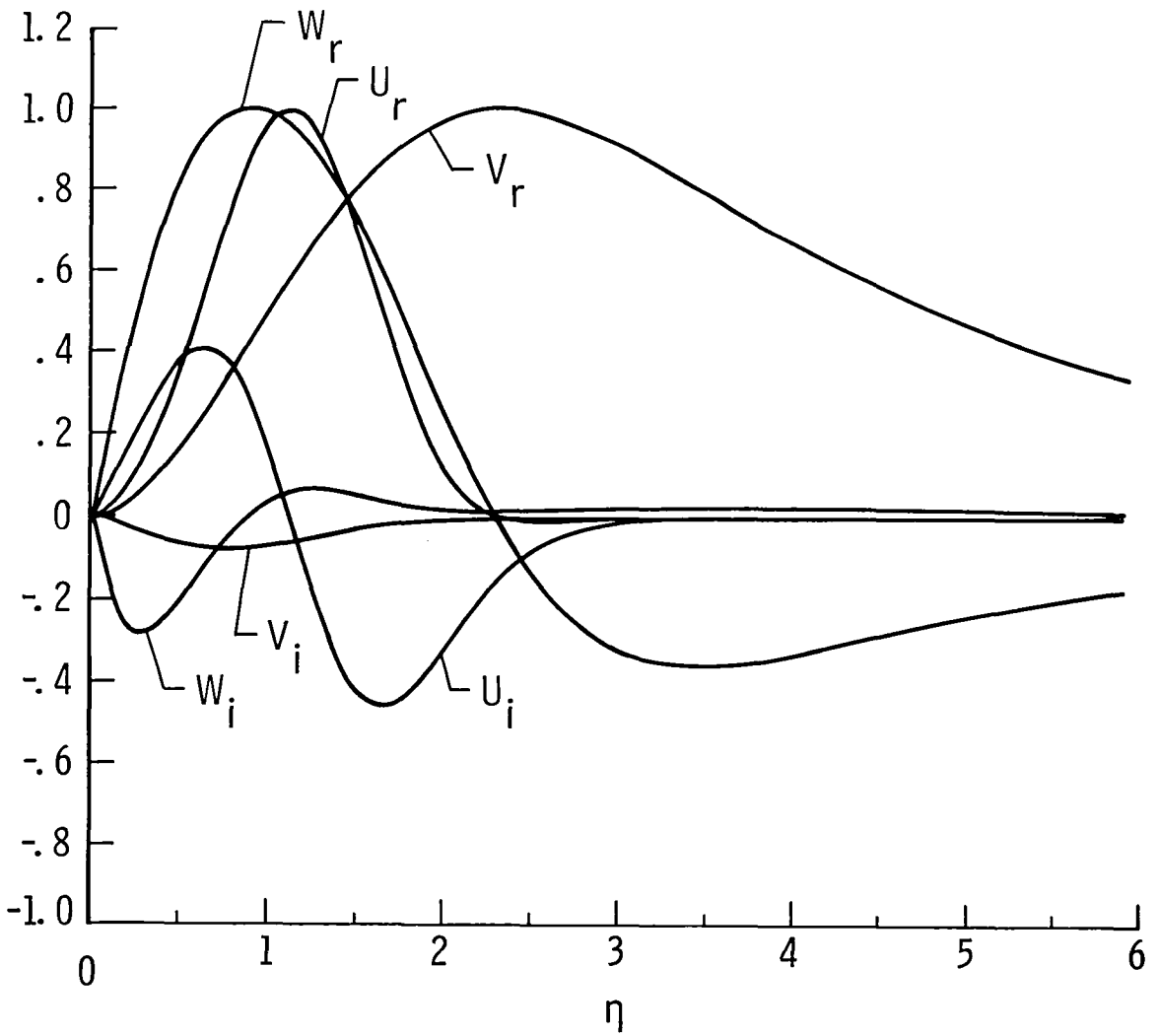
Figure 2e
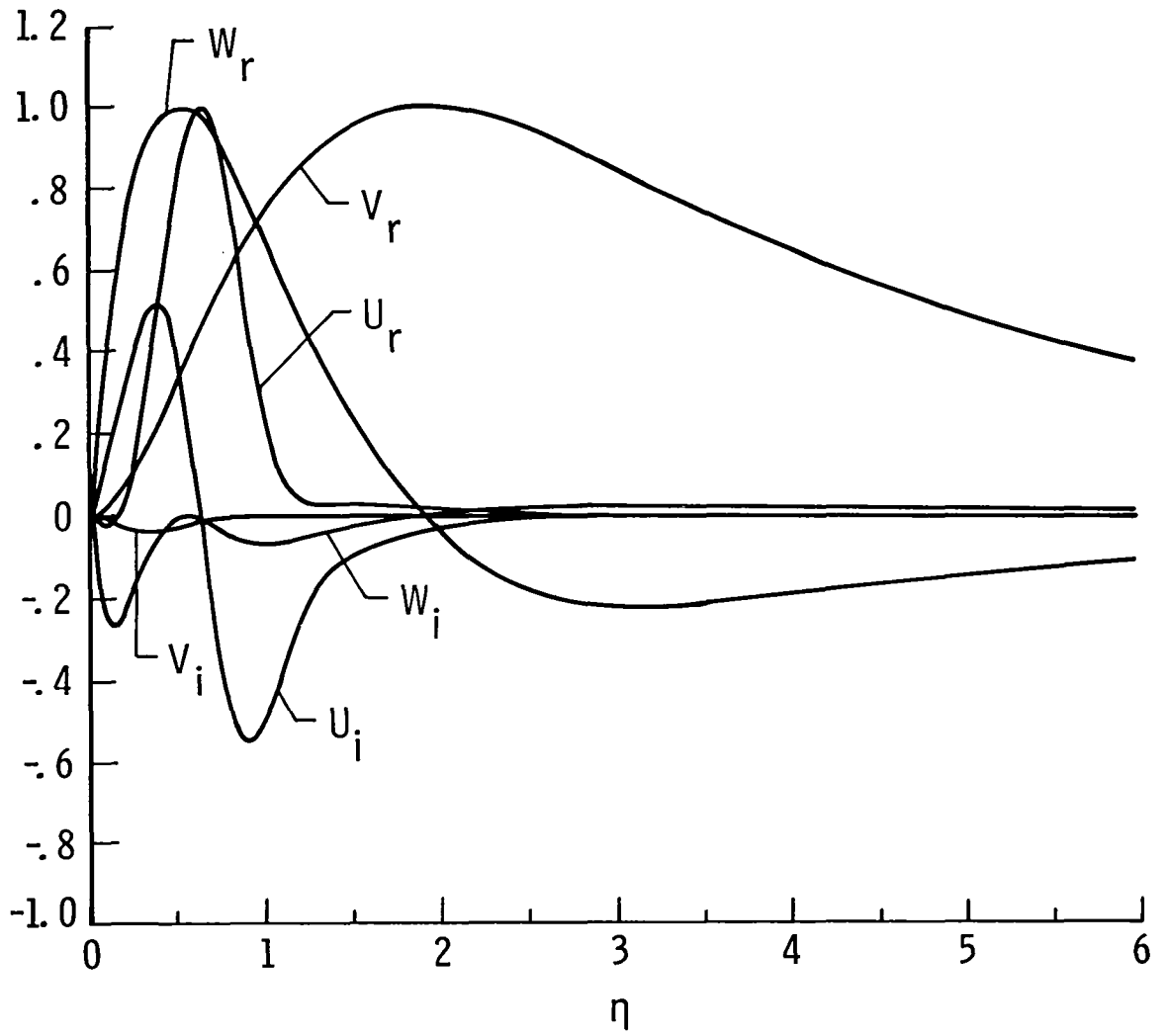
Figure 3

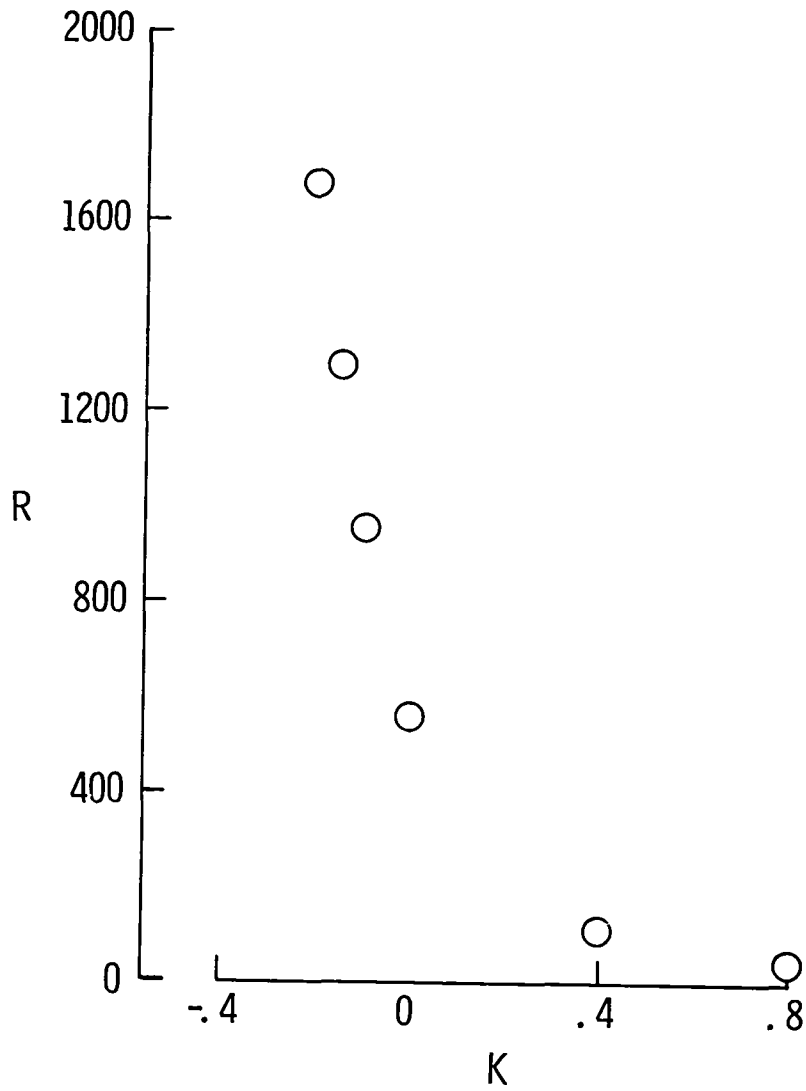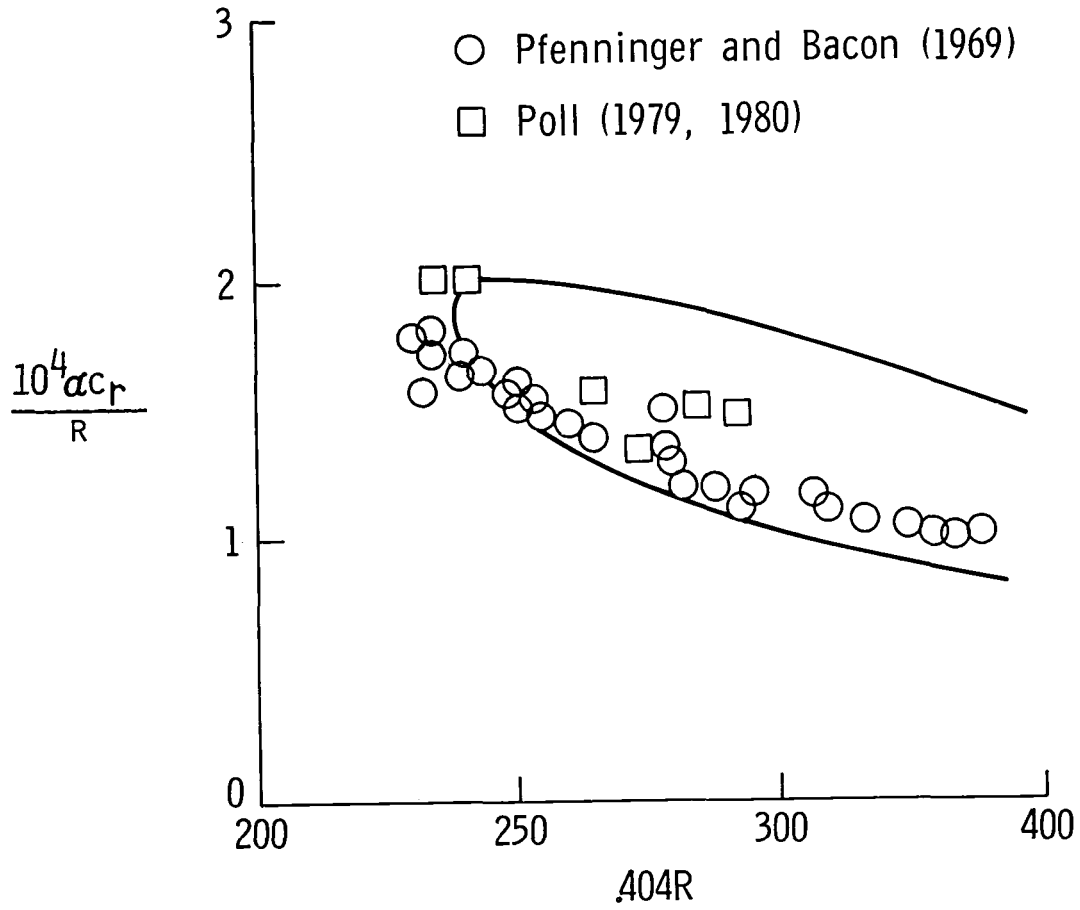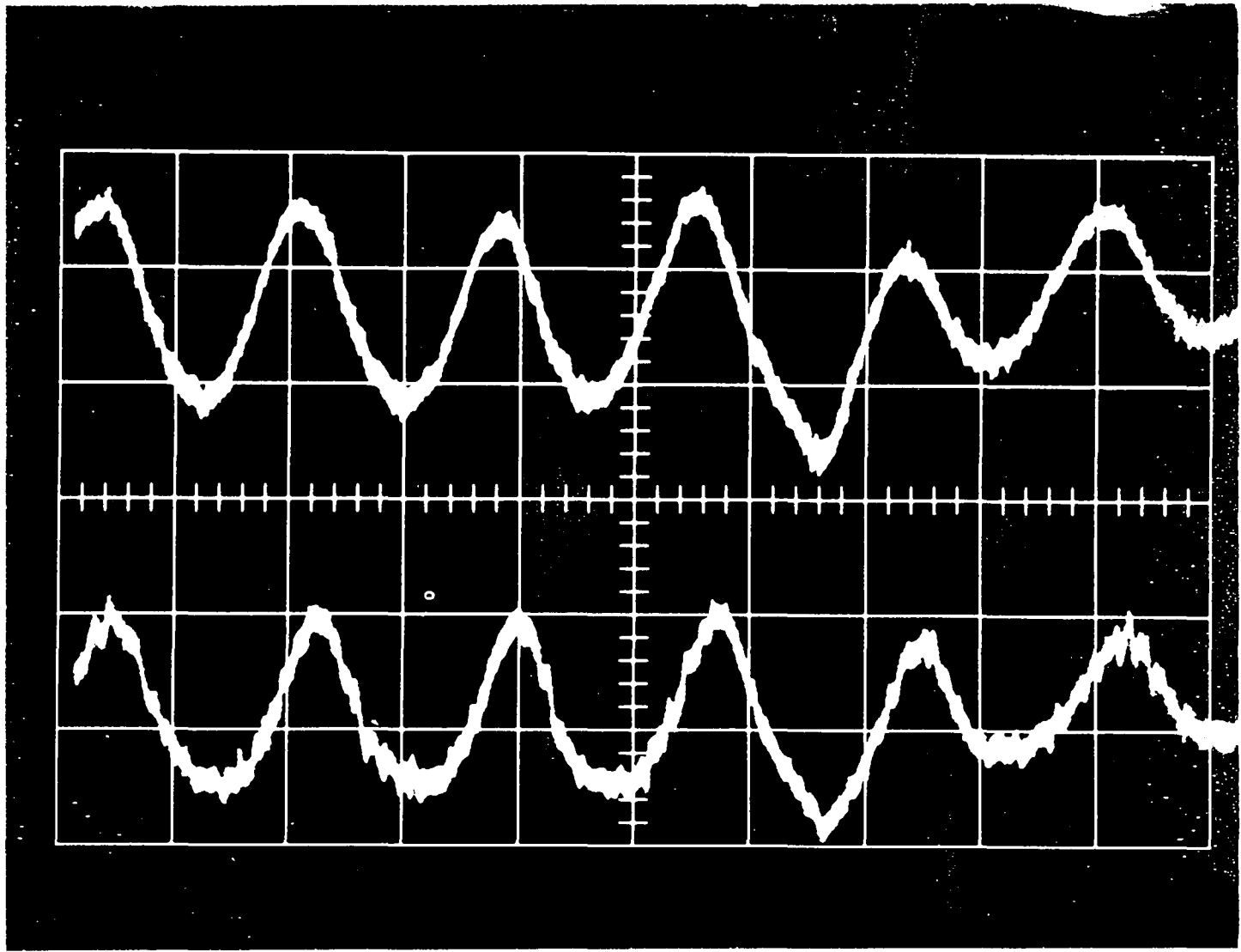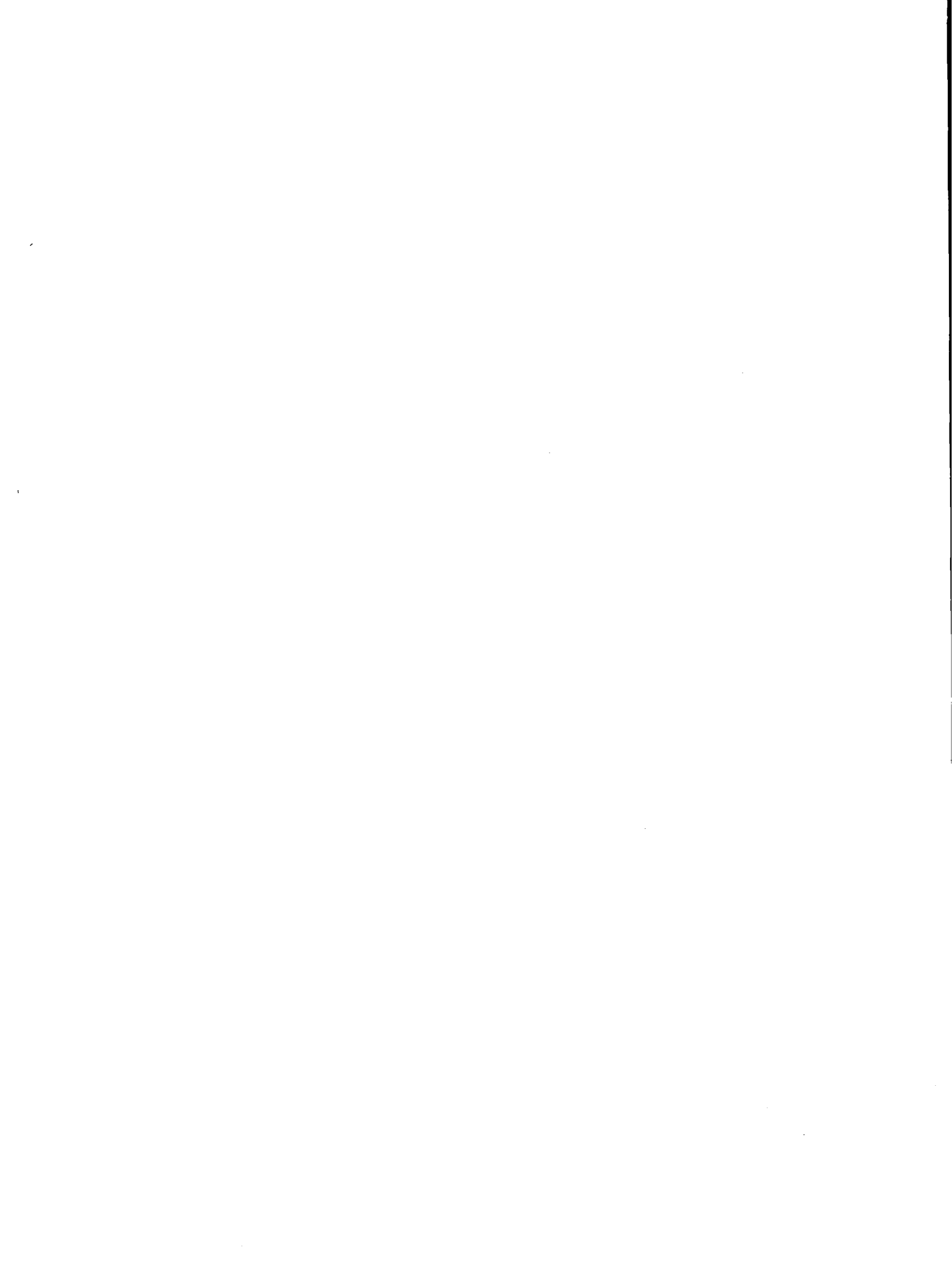Figure 4

Figure 5

1. Report No. NASA CR-172300	2. Government Accession No.	3. Recipient's Catalog No.
4. Title and Subtitle On the Stability of an Infinite Swept Attachment Line Boundary Layer		5. Report Date February 1984
		6. Performing Organization Code
7. Author(s) P. Hall*, M. R. Mallik**, D. I. A. Poll†		8. Performing Organization Report No. 84-5
9. Performing Organization Name and Address Institute for Computer Applications in Science and Engineering Mail Stop 132C, NASA Langley Research Center Hampton, VA 23665		10. Work Unit No.
		11. Contract or Grant No. NAS1-17070, NAS1-16916, NAS1-14605
12. Sponsoring Agency Name and Address National Aeronautics and Space Administration Washington, D.C. 20546		13. Type of Report and Period Covered contractor report
		14. Sponsoring Agency Code

16. Abstract

   The instability of an infinite swept attachment line boundary layer is considered in the linear regime. The basic three-dimensional flow is shown to be susceptible to travelling wave disturbances which propagate along the attachment line. The effect of suction on the instability is discussed and the results suggest that the attachment line boundary layer on a swept wing can be significantly stabilized by extremely small amounts of suction. The results obtained are in excellent agreement with the available experimental observations.

17. Key Words (Suggested by Author(s)) boundary layer instability	18. Distribution Statement 02 Aerodynamics 34 Fluid Mechanics and Heat Transfer Unclassified-Unlimited	
19. Security Classif. (of this report) Unclassified	20. Security Classif. (of this page) Unclassified	21. No. of Pages 45	22. Price A03